



# Simultaneous Observations of p-mode Light Walls and Magnetic Reconnection Ejections above Sunspot Light Bridges

Yijun Hou<sup>1,2</sup> , Jun Zhang<sup>1,2</sup>, Ting Li<sup>1,2</sup> , Shuhong Yang<sup>1,2</sup> , and Xiaohong Li<sup>1,2</sup>

<sup>1</sup> Key Laboratory of Solar Activity, National Astronomical Observatories, Chinese Academy of Sciences, Beijing 100012, China  
[yijunhou@nao.cas.cn](mailto:yijunhou@nao.cas.cn), [zjun@nao.cas.cn](mailto:zjun@nao.cas.cn)

<sup>2</sup> University of Chinese Academy of Sciences, Beijing 100049, China

Received 2017 July 14; revised 2017 September 21; accepted 2017 September 25; published 2017 October 9

## Abstract

Recent high-resolution observations from the *Interface Region Imaging Spectrograph* reveal bright wall-shaped structures in active regions (ARs), especially above sunspot light bridges. Their most prominent feature is the bright oscillating front in the 1400/1330 Å channel. These structures are named light walls and are often interpreted to be driven by p-mode waves. Above the light bridge of AR 12222 on 2014 December 06, we observed intermittent ejections superimposed on an oscillating light wall in the 1400 Å passband. At the base location of each ejection, the emission enhancement was detected in the *Solar Dynamics Observatory* 1600 Å channel. Thus, we suggest that in wall bases (light bridges), in addition to the leaked p-mode waves consistently driving the oscillating light wall, magnetic reconnection could happen intermittently at some locations and eject the heated plasma upward. Similarly, in the second event occurring in AR 12371 on 2015 June 16, a jet was simultaneously detected in addition to the light wall with a wave-shaped bright front above the light bridge. At the footpoint of this jet, lasting brightening was observed, implying magnetic reconnection at the base. We propose that in these events, two mechanisms, p-mode waves and magnetic reconnection, simultaneously play roles in the light bridge, and lead to the distinct kinetic features of the light walls and the ejection-like activities, respectively. To illustrate the two mechanisms and their resulting activities above light bridges, in this study we present a cartoon model.

**Key words:** Sun: activity – Sun: atmosphere – Sun: oscillations – Sun: UV radiation – sunspots

**Supporting material:** animations

## 1. Introduction

Sunspots are manifestations of solar magnetic field concentrations on the solar surface (Solanki 2003). The normal convective transports of plasma and energy are suppressed by the strong magnetic field in the sunspot umbra (Gough & Tayler 1966). Within the umbra, some bright structures exist as the result of incompletely inhibited convection, of which light bridges are the most prominent representatives (Borrero & Ichimoto 2011). Light bridges penetrate into the dark umbra, and strong ones can even separate the umbra completely. Previous studies showed that the light bridges have generally weaker and more inclined magnetic fields than the neighboring strong and vertical umbral fields, forming a magnetic canopy (Lites et al. 1991; Ruedi et al. 1995; Jurčák et al. 2006). Recently, observations and simulations revealed the existence of weakly twisted and emerging magnetic fields in the light bridge (Louis et al. 2015; Toriumi et al. 2015a, 2015b; Yuan & Walsh 2016).

Due to the divergence between the magnetic fields of light bridges and those of ambient umbra, some dynamic phenomena have been observed above light bridges, such as jets and surges (Roy 1973; Asai et al. 2001; Shimizu et al. 2009; Robustini et al. 2016; Bharti et al. 2017; Song et al. 2017), brightenings in the 1600 or 1400 Å ultraviolet (UV) and G-band channels (Berger & Berdyugina 2003; Tian et al. 2014b; Felipe et al. 2017), and light walls (Yang et al. 2015, 2016, 2017; Hou et al. 2016a, 2016b). In the H $\alpha$  channel, Asai et al. (2001) detected intermittent and recurrent plasma ejections above a light bridge. Small, newly emerging magnetic flux was considered to be essential for these surges. Shimizu et al. (2009) observed long-lasting chromospheric plasma ejections along the edge of a light bridge intermittently for

more than one day. They proposed that highly twisted magnetic flux tubes were trapped below a cusp-shaped magnetic structure along the light bridge, reconnecting with pre-existing vertical umbral fields. Similarly, Robustini et al. (2016, 2017) also reported fan-shaped (peacock) jets above a light bridge with H $\alpha$  observations and interpreted magnetic reconnection as the driver of these jets. With the high-resolution observations from the *Interface Region Imaging Spectrograph* (IRIS; De Pontieu et al. 2014) and the *New Vacuum Solar Telescope* (NVST; Liu et al. 2014) in China, Yang et al. (2015) reported oscillating bright structures with a bright front above a light bridge in the 1330 Å channel and named it a light wall. They suggested that the light wall was driven by leaked p-mode waves from the sub-photosphere. Independently, Bharti (2015) reported the same event and speculated that leakage of waves through the light bridge may be responsible for the coordinated behavior of neighboring oscillating structures. Recently, Zhang et al. (2017) analyzed IRIS spectral data of an oscillating wall above a light bridge and proposed that these surge-like oscillations result from shock waves generated by the upward p-mode.

As mentioned above, almost all the reported ejection-like activities above light bridges were explained by the magnetic reconnection. As for the light walls recently detected in IRIS 1400/1330 Å channels, they normally performed oscillating motions with bright front and were explained by the p-mode waves. Recently, we find that in some events, two mechanisms of p-mode waves and magnetic reconnection simultaneously play roles in the light bridge, leading to the distinct kinetic characteristics of the light walls and the ejection-like activities, respectively. In the present study, we

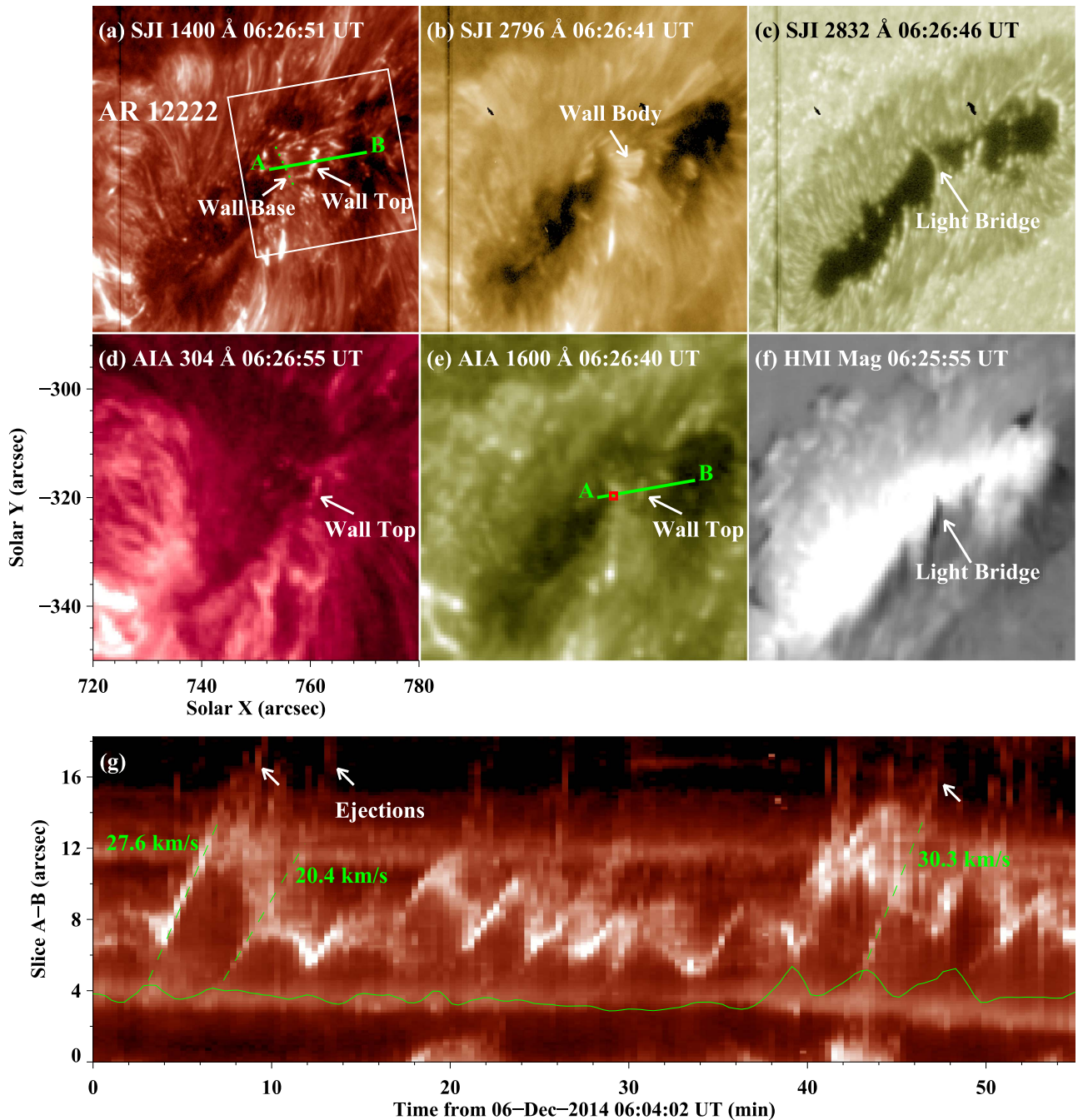


**Figure 1.** Panels (a)–(f): multi-wavelength (E)UV observations and a *SDO*/HMI LOS magnetogram displaying the targeted region in AR 12222 on 2014 December 06. The bright base and top of the light wall are denoted by the green dotted line and white arrows in panel (a). The white square in panel (a) outlines the FOV of Figure 2. The green “A–B” lines in panels (a) and (e) mark the cut position for the time–space plot exhibited in panel (g). The white arrows in panels (b), (d), and (e) denote the wall body in the 2796 Å image and the wall top in the 304 and 1600 Å passbands, respectively. The white arrows in panels (c) and (f) mark the light bridge. Panel (g): time–space plot along slice “A–B” in the 1400 Å channel. The green solid curve delineates the variation of mean emission strength in the 1600 Å passband within the region outlined by the small red square in panel (e), where the slice and the wall base intersect. The green dashed lines label the trajectories of the ejections before their arrivals in the light wall top, and the white arrows indicate the ejections above the wall top.

(An animation of this figure is available.)

analyze two sample events and propose a cartoon model for visualization.

## 2. Observations and Data Analysis

Our study mainly reports two events where the p-mode waves and magnetic reconnection simultaneously work in the

light bridge. The first event took place in active region (AR) NOAA 12222 on 2014 December 6. It was observed by *IRIS* from 06:03:46 UT to 07:01:53 UT with a spatial sampling of  $0''.166 \text{ pixel}^{-1}$  and a cadence of 21 s. We mainly use the slit-jaw images (SJIs) of the 1400, 2796, and 2832 Å passbands. The 1400 Å channel contains emission from the Si IV 1394/1403 Å lines formed in the low transition region ( $10^{4.9}$  K; Li et al. 2014;

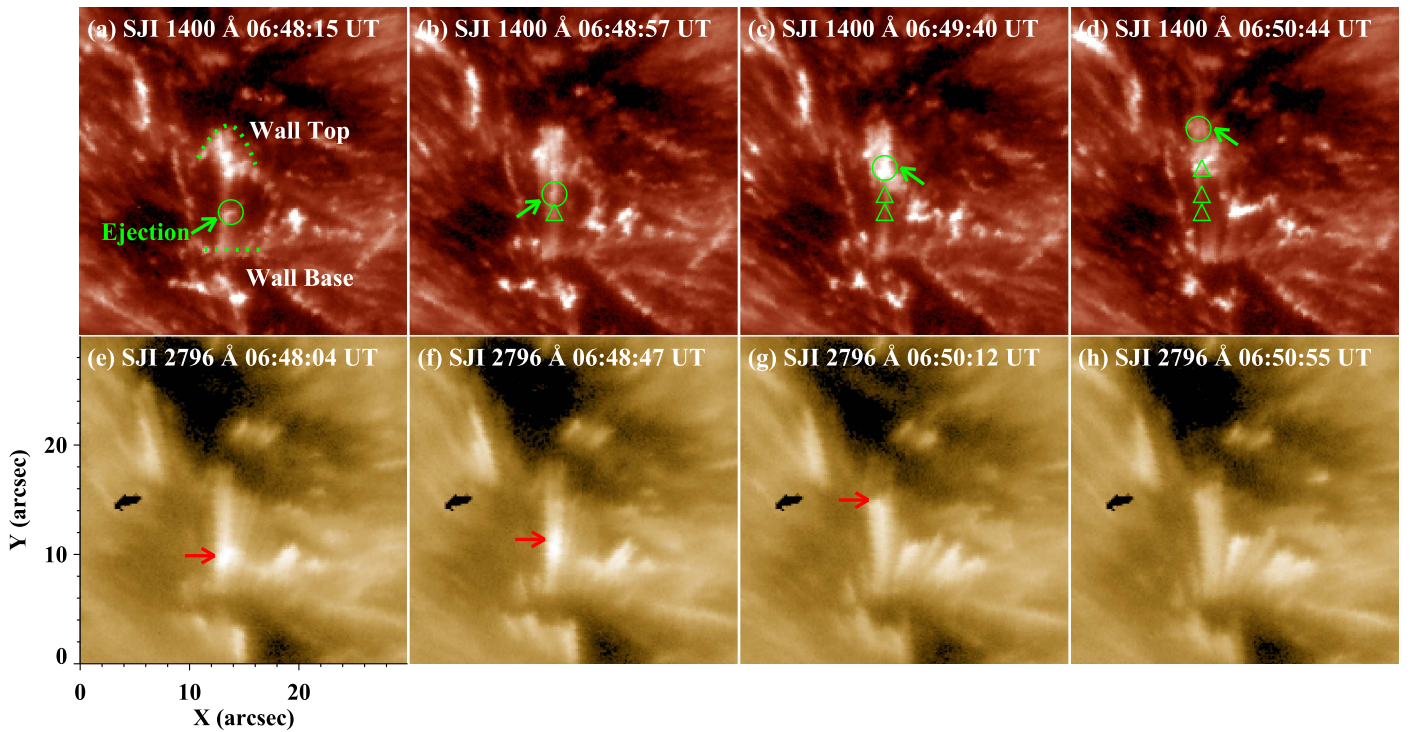


**Figure 2.** Panels (a)–(d): sequence of *IRIS* 1400 Å SJIs showing one process of the ejection moving upward from the wall base (see the green line in panel (a)) until escaping from the wall top (see the green curve in panel (a)). The green arrows and circles outline the locations of the ejections at corresponding times in each panel, while the green triangles mark their locations at the former moments. Panels (e)–(h): corresponding 2796 Å SJIs exhibiting the ejection motion in a cooler channel. The red arrows denote the positions of the ejection at different times.

Tian et al. 2014a) and the UV continuum emission. The 2796 Å channel is dominated by the Mg II k 2796 Å line emission formed in the upper chromosphere ( $10^{4.0}$  K). And the 2832 Å passband samples the wing of Mg II 2830 Å emission in the upper photosphere. For the second event occurring in AR 12371 on 2015 June 19, we take two series of 1400 Å and 2832 Å SJIs from 11:33:32 UT to 16:59:40 UT. The data have a spatial size of  $0''.333 \text{ pixel}^{-1}$  and a cadence of 20 s. All the employed data are level 2, where dark current subtraction, flat-field, geometrical, and orbital variation corrections have been applied (De Pontieu et al. 2014).

The Atmospheric Imaging Assembly (AIA; Lemen et al. 2012) on board the *Solar Dynamics Observatory* (SDO; Pesnell et al. 2012) observes the multi-layered solar atmosphere in 10 (E)UV channels with a cadence of (12)24 s and a pixel size of  $0''.6$ . Here, we focus on the observations of AIA 171, 304, and 1600 Å for the manifestations of the light walls in different passbands. Moreover, the full-disk line-of-sight (LOS) magnetograms from the Helioseismic and Magnetic Imager (HMI; Schou et al. 2012), with a cadence of 45 s and a sampling of  $0''.5 \text{ pixel}^{-1}$ , are also applied.

### 3. Results

The first event of interest happened above a light bridge in the main sunspot of NOAA AR 12222 when this AR approached the solar southwest limb on 2014 December 06. Figure 1 displays the *IRIS* and *SDO* observations of this event (also see movie1.mp4). The 2832 Å SJI in panel (c) shows that a light bridge separated the sunspot umbra completely at 06:26:46 UT (see the white arrow). Above this light bridge, a light wall was detected clearly in the SJI of 1400 Å with the wall

base rooted in the light bridge and the bright front (wall top) extending to the west (panel (a)). The light wall manifested as a bright wall body without a bright front in the 2796 Å image (panel (b)). Panel (d) exhibits the wall in the 304 Å channel, and it is clear that the wall top has high emission, while the emissions at both the base and body are quite weak. The manifestation of the light wall in the 1600 Å image of panel (e) is similar to that in the 1400 Å channel. Superimposed on the oscillation behavior of the light wall top, intermittent and recurrent plasma ejections were observed. To investigate the kinetic characteristics of the light wall, as well as the ejections, we derive a time–space plot from a sequence of 1400 Å SJIs along the slice “A–B” marked in panel (a), and display it in panel (g). As shown in the time–space plot, some plasma ejections intermittently moved upward from the wall base and eventually escaped from the wall top (see the white arrows in panel (g)). We label three ejections with green dashed lines in panel (g) and estimate their projected velocities as  $27.6 \text{ km s}^{-1}$ ,  $20.4 \text{ km s}^{-1}$ , and  $30.3 \text{ km s}^{-1}$ , respectively. Meanwhile, the rising velocity of the wall top is approximated with a mean value of  $14.1 \text{ km s}^{-1}$ . We also check the mean emission strength in 1600 Å passband around their base location. The green solid curve in panel (g) delineates variation of the mean emission strength within the selected base region (see the red square in panel (e)). Taking the average value of a light wall as  $I_0$ , then we measure the value of ejections as about  $3 I_0$ . It is shown that one ejection lasted for about 6 minutes and almost each ejection corresponded to an emission peak in its base location.

In Figure 2, a process of the ejections is examined. We cut out a smaller field of view (FOV) in the *IRIS* 1400 Å SJIs (see the white square in Figure 1(a)) and rotate them  $80^\circ$  anticlockwise; the rotated SJIs are shown in Figures 2(a)–(d).

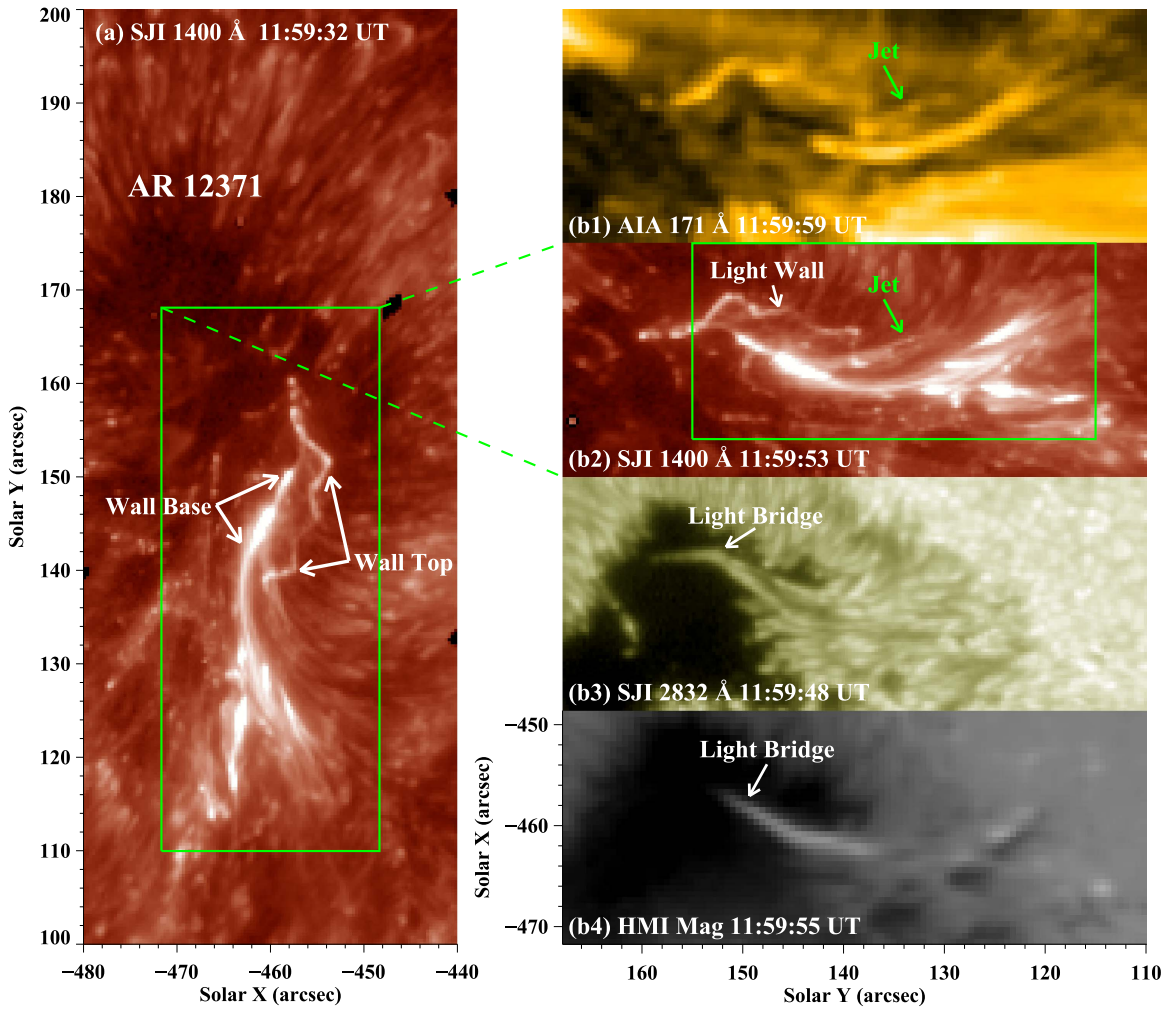


**Figure 3.** Panel (a): *IRIS* 1400 Å SJI displaying the overview of the second event of interest in AR 12371 on 2015 June 19. Panels (b1)–(b4): AIA 171 Å image, *IRIS* SJIs of 1400 and 2832 Å, and HMI LOS magnetogram exhibiting the jet, light wall, and light bridge, as well as their underlying magnetic fields. The green arrows in panels (b1) and (b2) denote the jet, and the white arrow in panel (b2) marks the light wall. They exist simultaneously above the sunspot light bridge (see the white arrows in panels (b3) and (b4)). The green rectangle in panel (b2) outlines the FOVs of Figures 4(a)–(d).

(An animation of this figure is available.)

From 06:48:15 UT to 06:50:44 UT, we track an ejected blob-like structure after its departure from the base until escaping from the wall top. This ejected structure moved upward with a mean speed of  $34.5 \text{ km s}^{-1}$  (see the green arrows and circles). In the corresponding 2796 Å SJIs shown in panels (e)–(h), the ejection appeared as a mass of brightening material and moved upward from the wall base to the wall top between 06:48:04 UT and 06:50:12 UT, which is consistent with the motion of ejected blob-like structure observed in the 1400 Å channel. In addition, we estimate the widths of the ejections above the light bridge to be about 1.5 Mm.

The second event took place above a sunspot light bridge within AR 12371 on 2015 June 19. Figure 3(a) displays the overview of this region in the *IRIS* 1400 Å channel. The light wall showed a bright base and a distinct wave-shaped bright front at 11:59:32 UT (see the white arrows). To exhibit the light wall more intuitively, we rotate the 1400 Å images 90° anticlockwise and expand part of this region (see the green rectangle), which is then shown in panels (b1)–(b4) (see the corresponding animation movie2.mp4). The 2832 Å SJI and HMI LOS magnetogram reveal that the light wall was rooted in a light bridge within a negative-polarity sunspot (panels (b3)–(b4)). In addition to the

light wall, a jet was simultaneously found to be rooting in the brightening wall base at 11:59:53 UT.

To investigate the evolution of this jet, we focus on a smaller region outlined by the green rectangle in Figure 3(b2). Figures 4(a)–(d) exhibit the temporal evolution of this jet in the 1400 Å passband. Above the light bridge, a light wall was detected with a wave-shaped front at 12:00:13 UT (panel (b)). In the southwest of the wall base, brightening appeared from 11:52 UT, where then a jet was formed (see the green arrows in panels (b)–(d)). The jet lasted for about half an hour, accompanied by the consistent brightening of base. The green arc-sector domain “C–D” in panel (a) approximates the trajectory of the jet. We make a time–space plot along this arc-sector domain; it is shown show in panel (e). After 11:52 UT, bright materials began to eject upward from the wall base, forming a jet with a lifetime of about 20 minutes. The projected velocity of this jet is about  $30 \text{ km s}^{-1}$ , while the mean rising velocity of the wall top is about  $12.5 \text{ km s}^{-1}$ .

#### 4. Summary and Discussion

Employing high-resolution observations from the *IRIS* and the *SDO*, we detect two events tracking the coexistence

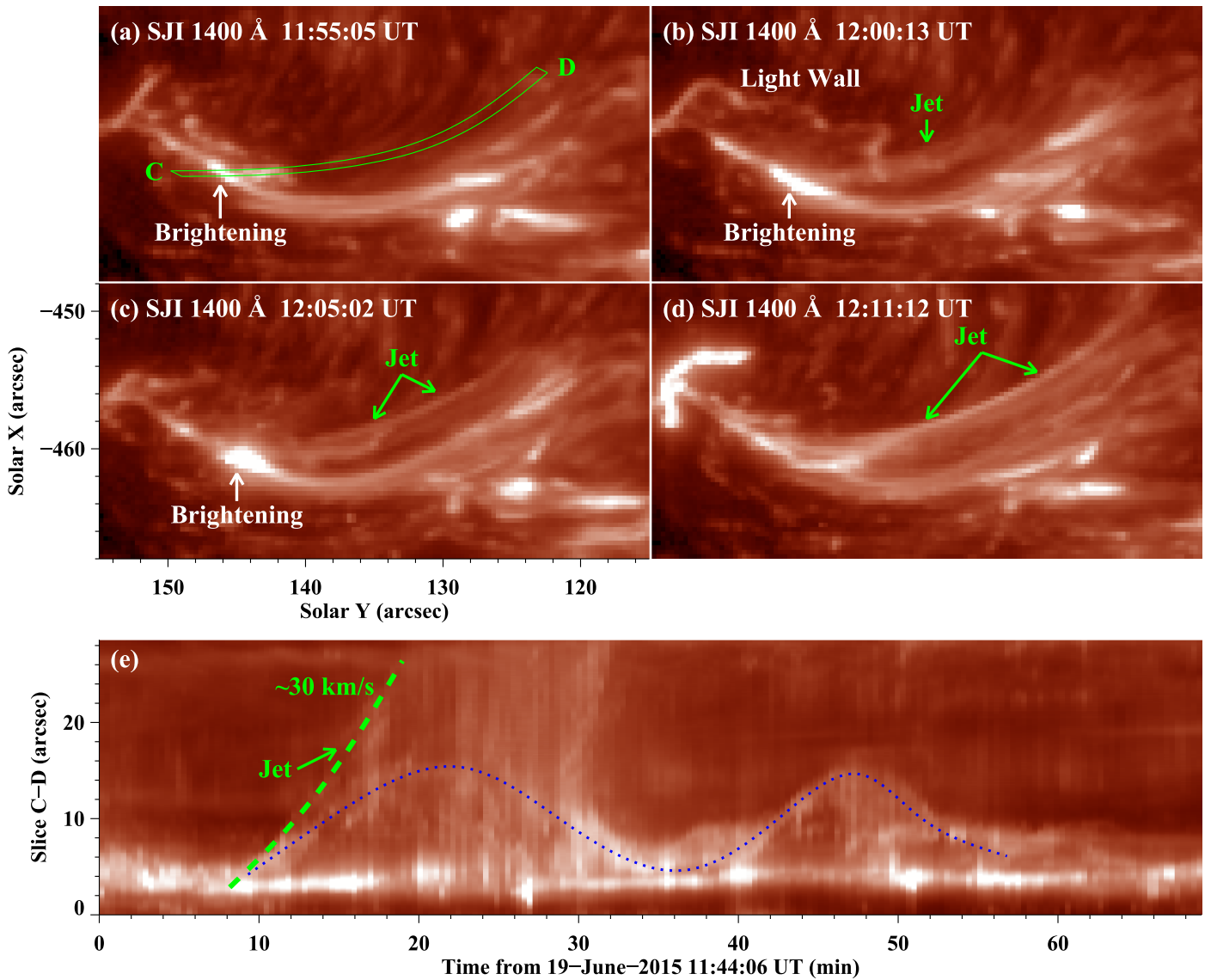


**Figure 4.** Panels (a)–(d): time sequence of *IRIS* 1400 Å images showing the evolution of the jet. The green arc-sector domain “C–D” in panel (a) is along the trajectory of the jet, and a time–space plot is made along this arc-sector domain. The white arrows mark the location of the brightening wall base, where the jet is triggered. The green arrows denote the jet in different phases during its development. Panel (e): time–space plot along the arc-sector domain “C–D” of panel (a) in the 1400 Å channel. The blue dotted curve delineates the top of the light wall, and the green dashed line approximates the trajectory of the jet.

between light walls and ejection-like activities above a light bridge. In the first event, which occurred in AR 12222 on 2014 December 06, an oscillating light wall was detected above a strong sunspot light bridge in the 1400 Å channel. Superimposed on the oscillation behavior of the light wall top, some plasma ejections intermittently moved upward from the wall base (light bridge) and eventually escaped from the wall top. These ejections corresponded well with emission enhancements in the wall base and had a mean projected velocity of about  $26 \text{ km s}^{-1}$  in the initial phase. The second event took place in the main sunspot of AR 12371 on 2015 June 16. Above the light bridge in this sunspot, the light wall was observed with a wave-shaped bright front. Additionally, a jet with a projected velocity of about  $30 \text{ km s}^{-1}$  was simultaneously detected, accompanied by the consistent brightening of the wall base in the 1400 Å passband.

In recent years, light walls have been reported in several works (Yang et al. 2015, 2016, 2017; Hou et al. 2016b, 2016a). In this study, the first event exhibited the intermittent ejections

superimposed on the light wall. Figure 1(g) shows that the upwardly propagating wall top is brighter than the falling one. It could be caused by the leaked p-mode waves, which nonlinearly steepen to form shocks, elevating and heating the chromospheric material. This observational fact further supports the scenario of p-mode leakage and the resultant shock propagation (De Pontieu et al. 2004; Morton 2012; Rouppe van der Voort & de la Cruz Rodríguez 2013; Zhang et al. 2017). Furthermore, checking the observations from AIA 1600 Å, we noted that there was enhanced emission in the base location corresponding to each ejection. In the 2796 and 1400 Å passbands, the ejections appeared as a mass of brightening material moving upward from the wall base. Thus, we suggest that in the light bridge, in addition to the leaked p-mode waves consistently driving and heating the chromospheric material to form the oscillating light wall, magnetic reconnection could happen intermittently in some locations and eject the heated plasma upward. Similarly, in the second event, a jet was simultaneously detected in addition to the light wall with a

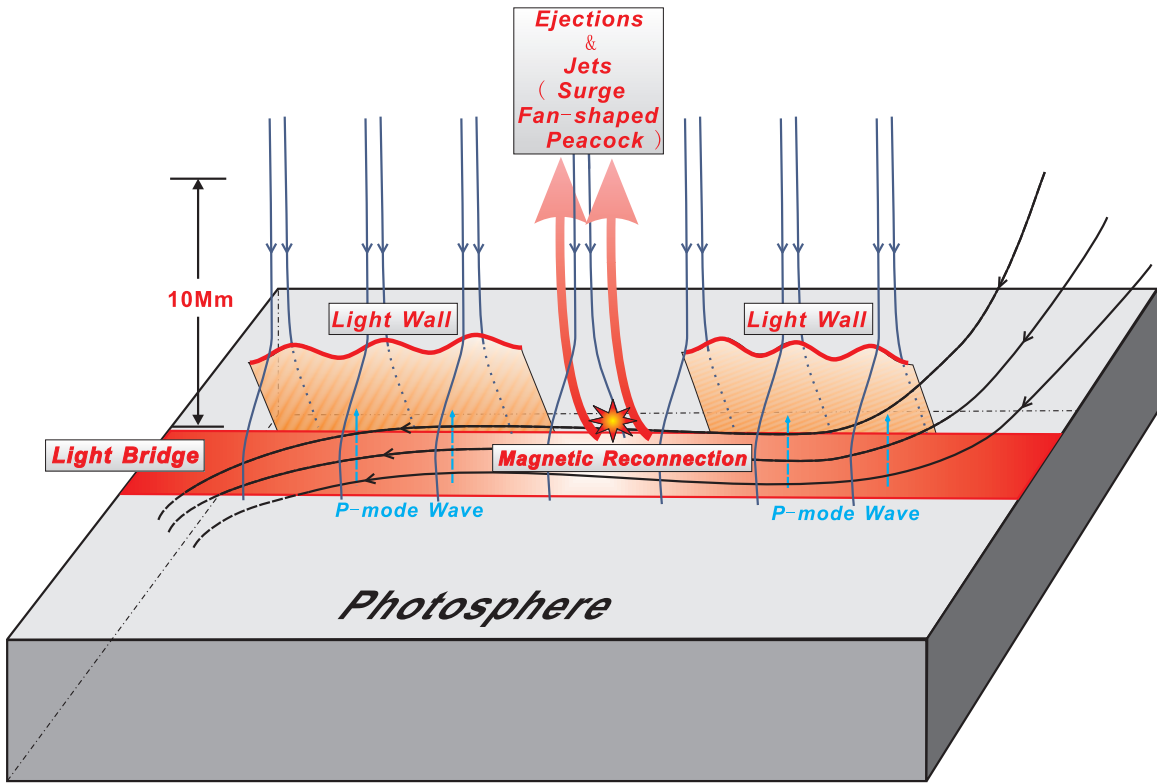


**Figure 5.** Schematic diagram illustrating the two mechanisms and their resulting activities above sunspot light bridges. The gray cube represents the space underneath the photosphere, above which the light bridge and associated dynamic activities are observed. The red rectangle approximates the map of the light bridge on the photosphere. The black curves delineate the horizontal magnetic field lines in the light bridge. The navy blue curves represent the vertical field lines around the light bridge, which perform a magnetic canopy in the lower section. The orange regions outline the light wall above the light bridge, under which the cyan arrows denote the p-mode waves propagating upward from the sub-photosphere. The red curves above the orange regions delineate the bright front of the light wall. The star symbol marks the site of magnetic reconnection, above which the ejections and jets are triggered and shown by large pink arrows.

wave-shaped bright front above the light bridge. At the footpoint of this jet, remarkable brightening was observed in the  $1400 \text{ \AA}$  channel that could be a signal of magnetic reconnection in the light bridge. We propose that in these events, two mechanisms of p-mode waves and magnetic reconnection simultaneously played roles in the light bridge, resulting in distinct kinetic features for the light walls and the ejection-like activities, respectively. We come to this conclusion based on the following points: (1) the light walls rise with a projected velocity of about  $10 \text{ km s}^{-1}$ , while the ejections rise with a velocity of about  $30 \text{ km s}^{-1}$ ; (2) compared to the light walls with typical heights of several Mm, jets have much larger heights of tens of Mm; (3) the lifetime of the ejections is about 10 minutes, while the light walls could exist for several hours (even up to several days in Hou et al. 2016a); (4) calculating the  $1600 \text{ \AA}$  intensity at the base location, if we take the average value of light walls as  $I_0$ , then the value of ejections is about  $3 I_0$ ; (5) differing from ejections that have typical base widths of about 1.5 Mm, the light walls are usually coherent above the light bridge over a spatial range of about tens of Mm (e.g., 10–20 Mm). Similar viewpoints have been mentioned in previous works (Morton 2012; Bharti 2015; Yang et al. 2015). Recently, Zhang et al. (2017) also claimed that their upcoming paper would reveal both shock-driven and reconnection-related surges in a single observation.

To illustrate the two mechanisms and their resulting activities above sunspot light bridges, we propose a cartoon model (Figure 5). The red rectangle approximates the map of the light bridge on the photosphere. The light bridge has

horizontal fields, above which a magnetic canopy exists (Leka 1997; Katsukawa et al. 2007; Lagg et al. 2014). Louis et al. (2014) proposed that the jets above the light bridge could be guided by the magnetic field lines. Similarly, the light walls outlined by the orange regions here are along the field lines rooted at the edge of the light bridge. The light walls are generally driven by the leaked p-mode waves from below the photosphere and have typical heights of several Mm. But in some locations of the light bridge, the magnetic reconnection takes place between the horizontal fields and the surrounding vertical fields. Then, the ejections or jets (surge, fan-shaped, and peacock) are triggered (Asai et al. 2001; Shimizu et al. 2009; Robustini et al. 2016). Note that in the case of an emerging magnetic field with a line-like shape, the magnetic reconnection could happen in a region of line shape and trigger light walls with heights of over 10 Mm (Hou et al. 2016b). It was reported that these light walls only displayed bright threads in the  $1400 \text{ \AA}$  passband. But in the  $H\alpha$  channel, they seemed to be composed of multiple bright and dark threads, which was similar to the fan-shaped (peacock) jets driven by reconnection that were studied in Robustini et al. (2016).

Ejection-like activities caused by magnetic reconnection have been observed with heights of tens of Mm above light bridges in many works. Although we speculate that beside these jets, light walls with typical heights of several Mm triggered by the p-mode waves usually coexist, these light walls could be easily overlooked due to much their smaller scales compared to the jets and the constraints of previous observations. Therefore, it is necessary for us to statistically

analyze the activities above light bridges and their magnetic circumstances in further studies.

The authors are grateful to the anonymous referee for valuable suggestions. These data are used courtesy of the *SDO* and *IRIS* science teams. *IRIS* is a NASA small explorer mission developed and operated by LMSAL with mission operations executed at the NASA Ames Research center and major contributions to downlink communications funded by ESA and the Norwegian Space Centre. This work is supported by the National Natural Science Foundations of China (11533008, 11673035, 11673034, and 11773039) and the Youth Innovation Promotion Association of CAS (2017078 and 2014043).

### ORCID iDs

Yijun Hou  <https://orcid.org/0000-0002-9534-1638>

Ting Li  <https://orcid.org/0000-0001-6655-1743>

Shuhong Yang  <https://orcid.org/0000-0002-6565-3251>

### References

- Asai, A., Ishii, T. T., & Kurokawa, H. 2001, *ApJL*, 555, L65  
 Berger, T. E., & Berdyugina, S. V. 2003, *ApJL*, 589, L117  
 Bharti, L. 2015, *MNRAS*, 452, L16  
 Bharti, L., Solanki, S. K., & Hirzberger, J. 2017, *A&A*, 597, A127  
 Borrero, J. M., & Ichimoto, K. 2011, *LRSP*, 8, 4  
 De Pontieu, B., Erdélyi, R., & James, S. P. 2004, *Natur*, 430, 536  
 De Pontieu, B., Title, A. M., Lemen, J. R., et al. 2014, *SoPh*, 289, 2733  
 Felipe, T., Collados, M., Kholenko, E., et al. 2017, *A&A*, in press (arXiv:1708.06133)  
 Gough, D. O., & Tayler, R. J. 1966, *MNRAS*, 133, 85  
 Hou, Y., Zhang, J., Li, T., et al. 2016a, *ApJL*, 829, L29  
 Hou, Y. J., Li, T., Yang, S. H., & Zhang, J. 2016b, *A&A*, 589, L7  
 Jurčák, J., Martínez Pillet, V., & Sobotka, M. 2006, *A&A*, 453, 1079  
 Katsukawa, Y., Yokoyama, T., Berger, T. E., et al. 2007, *PASJ*, 59, S577  
 Lagg, A., Solanki, S. K., van Noort, M., & Danilovic, S. 2014, *A&A*, 568, A60  
 Leka, K. D. 1997, *ApJ*, 484, 900  
 Lemen, J. R., Title, A. M., Akin, D. J., et al. 2012, *SoPh*, 275, 17  
 Li, L. P., Peter, H., Chen, F., & Zhang, J. 2014, *A&A*, 570, A93  
 Lites, B. W., Bida, T. A., Johannesson, A., & Scharmer, G. B. 1991, *ApJ*, 373, 683  
 Liu, Z., Xu, J., Gu, B.-Z., et al. 2014, *RAA*, 14, 705  
 Louis, R. E., Beck, C., & Ichimoto, K. 2014, *A&A*, 567, A96  
 Louis, R. E., Bellot Rubio, L. R., de la Cruz Rodríguez, J., Socas-Navarro, H., & Ortiz, A. 2015, *A&A*, 584, A1  
 Morton, R. J. 2012, *A&A*, 543, A6  
 Pesnell, W. D., Thompson, B. J., & Chamberlin, P. C. 2012, *SoPh*, 275, 3  
 Robustini, C., Leenaarts, J., & de la Cruz Rodríguez, J. 2017, arXiv:1709.03864  
 Robustini, C., Leenaarts, J., de la Cruz Rodríguez, J., & Rouppe van der Voort, L. 2016, *A&A*, 590, A57  
 Rouppe van der Voort, L., & de la Cruz Rodríguez, J. 2013, *ApJ*, 776, 56  
 Roy, J. R. 1973, *SoPh*, 28, 95  
 Ruedi, I., Solanki, S. K., & Livingston, W. 1995, *A&A*, 302, 543  
 Schou, J., Scherrer, P. H., Bush, R. I., et al. 2012, *SoPh*, 275, 229  
 Shimizu, T., Katsukawa, Y., Kubo, M., et al. 2009, *ApJL*, 696, L66  
 Solanki, S. K. 2003, *A&ARv*, 11, 153  
 Song, D., Chae, J., Yurchyshyn, V., et al. 2017, *ApJ*, 835, 240  
 Tian, H., DeLuca, E., Reeves, K. K., et al. 2014a, *ApJ*, 786, 137  
 Tian, H., Kleint, L., Peter, H., et al. 2014b, *ApJL*, 790, L29  
 Toriumi, S., Cheung, M. C. M., & Katsukawa, Y. 2015a, *ApJ*, 811, 138  
 Toriumi, S., Katsukawa, Y., & Cheung, M. C. M. 2015b, *ApJ*, 811, 137  
 Yang, S., Zhang, J., & Erdélyi, R. 2016, *ApJL*, 833, L18  
 Yang, S., Zhang, J., Erdélyi, R., et al. 2017, *ApJL*, 843, L15  
 Yang, S., Zhang, J., Jiang, F., & Xiang, Y. 2015, *ApJL*, 804, L27  
 Yuan, D., & Walsh, R. W. 2016, *A&A*, 594, A101  
 Zhang, J., Tian, H., He, J., & Wang, L. 2017, *ApJ*, 838, 2